CHAPTER 35

RIP - CURRENTS

by

Edward K. Noda
Tetra Tech, Inc.
Pasadena, California

ABSTRACT

The generation and stabilization of rip - current circulation patterns is considered herein. An analytic model is developed to simulate the wave hydrodynamic processes in the nearshore zone, strongly influenced by the local bottom topography. The wave induced nearshore circulation pattern is computed and the results compared to prototype field data.

INTRODUCTION

One of the most common hydrodynamic features of the nearshore zone is the generation and stabilization of rip - current circulation patterns. While the rip - current phenomenon is well known visually, its generating mechanism is not well understood. This understanding of the characteristics of rip - current processes and nearshore circulation is an important link in analyzing the complicated interaction between hydrodynamics and sedimentation in the coastal zone.

Presently there are two theories concerning the generation of nearshore rip - current patterns. Bowen (1) proposed a driving mechanism consisting of a longshore variation of average wave height across a rip - current cell with waves impinging normally onto a plane beach. Bowen suggested that this longshore variation of wave height might be due to edge waves. While the circulation patterns appear qualitatively realistic, the quantitative results are not so optimistic.

Sonu (6) suggests that rip - current circulation patterns are strongly influenced by the local bottom topography. The coupling of the wave characteristics and bottom topography produced the necessary driving mechanism. A schematic description of the types of stream line patterns occurring in the nearshore zone is described in Figure 1 from Sonu. Detailed quantitative field data is shown in Figures 5 and 8 to correlate with Figure 1.

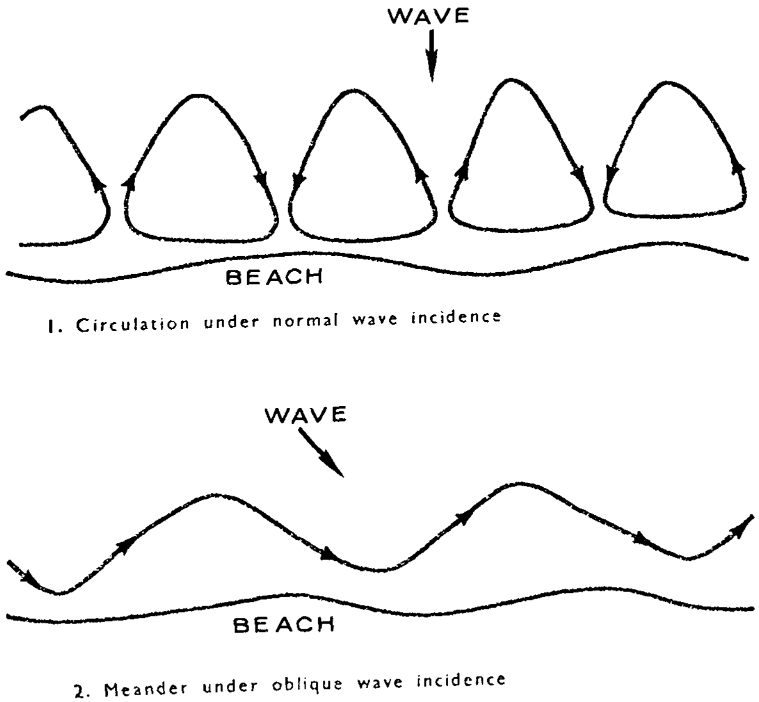

Figure 1: Schematic Display of Current Patterns due to Normal and Oblique Wave Incidence [Sonu (6)].

In the following analysis an analytic model is developed to correlate rip - current patterns with wave characteristics affected by the local non-uniform bottom topography.

THEORY

Figure 2 describes the coordinate system. To obtain the wave height and direction field the "geometrics optics" approximation is utilized where the ray equations describing the x, y and θ values along the ray are

$$\frac{dx}{ds} = \cos\theta \tag{1}$$

$$\frac{dy}{ds} = \sin\theta \tag{2}$$

and

$$\frac{d\theta}{ds} = \frac{1}{c}\left[\sin\theta\frac{\partial c}{\partial x} - \cos\theta\frac{\partial c}{\partial y}\right] \tag{3}$$

where s is displacement along the ray and c is the wave celerity defined by

$$c = \frac{gT}{2\pi}\tanh\left(\frac{2\pi d}{cT}\right) \tag{4}$$

Eqs. (1) to (3) are kinematic equations describing the ray location. To find the wave height, the intensity equation as given by Munk and Arthur (5) is used

$$\frac{d^2\beta}{ds^2} + p(s)\frac{d\beta}{ds} + q(s)\beta = 0 \tag{5}$$

where

$$p(s) = -\cos\theta\left[\frac{1}{c}\frac{\partial c}{\partial x}\right] - \sin\theta\left[\frac{1}{c}\frac{\partial c}{\partial y}\right] \tag{6}$$

and

$$q(s) = \sin^2\theta\left[\frac{1}{c}\frac{\partial^2 c}{\partial x^2}\right] - 2\sin\theta\cos\theta\left[\frac{1}{c}\frac{\partial^2 c}{\partial x\partial y}\right] + \cos^2\theta\left[\frac{1}{c}\frac{\partial^2 c}{\partial y^2}\right] \tag{7}$$

The wave height due to refraction alone is then given by

$$H = \frac{Ho}{\sqrt{\beta}} \tag{8}$$

where Ho is the deep water wave height.

To solve Eqs. (1) to (4) a 4th order Runga-Kutta technique is utilized where

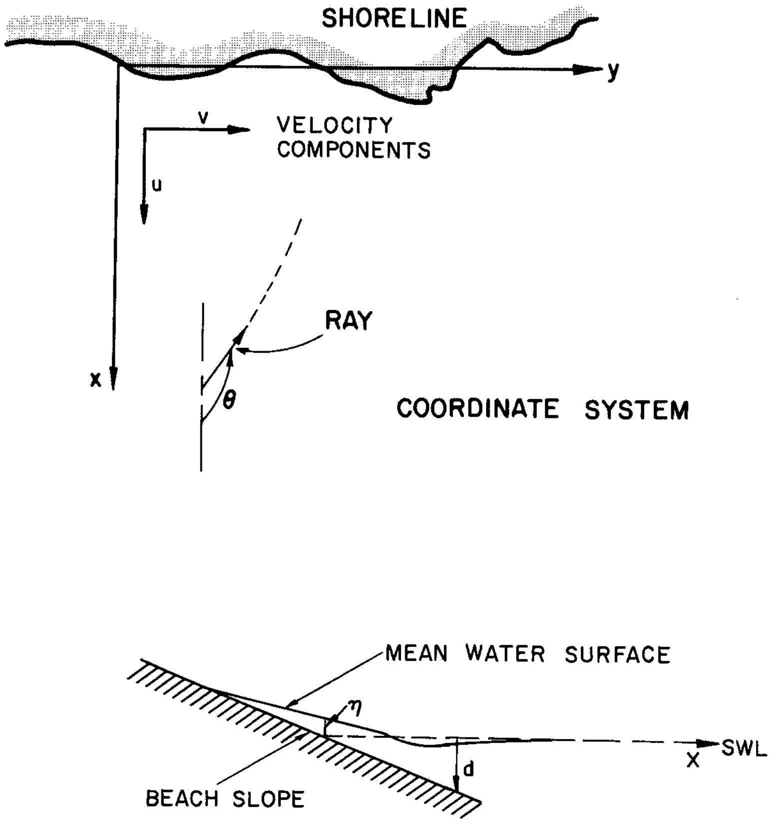

Figure 2: Coordinate System

Eq. (4) is divided into two (2) first order equations. Thus, the simultaneous solution of five (5) first order equations yields the wave height and direction field.

As the wave propagates into shore, the effects of refraction and shoaling can produce a breaking wave. Consequently, an empirical breaking criterion is imposed. From Miche (4) the limiting wave steepness is

$$\frac{H_b}{L_b} = 0.142 \tanh \left(\frac{2\pi d_b}{L_b}\right) \tag{9}$$

although an examination of experimental data of waves breaking over a horizontal bottom by LeMéhauté and Koh (2) indicates a better criterion is

$$\frac{H_b}{L_b} = 0.12 \tanh \left(\frac{2\pi d_b}{L_b}\right) \tag{10}$$

For the following analysis Eq. (10) has been utilized. Note that breaking characteristics may be influenced by "local" bottom slope which is not considered herein.

Once the wave height and direction fields are known, the nearshore circulation pattern can then be computed. To facilitate the analysis, the momentum and continuity equations have been vertically integrated and the time dependent and nonlinear terms neglected to yield

$$g\frac{\partial \eta}{\partial x} = M_x - F_x \tag{11}$$

$$g\frac{\partial \eta}{\partial y} = M_y - F_y \tag{12}$$

and the continuity equation

$$\frac{\partial [u(\eta+d)]}{\partial x} + \frac{\partial [v(\eta+d)]}{\partial y} = 0 \tag{13}$$

where the radiation stress terms are [Longuet-Higgins and Stewart (3)]

$$M_x = -\frac{1}{\rho(d+\eta)} \left[\frac{\partial \sigma_{xx}}{\partial x} + \frac{\partial \tau_{xy}}{\partial y}\right] \tag{14}$$

$$M_y = -\frac{1}{\rho(d+\eta)} \left[\frac{\partial \sigma_{yy}}{\partial y} + \frac{\partial \tau_{xy}}{\partial y}\right]$$

and the friction terms are

$$F_x = \frac{2cuH}{(\eta+d)T \sinh kd} \tag{15}$$

$$F_y = \frac{2cvH}{(\eta + d)T \sinh kd} \tag{16}$$

where

$$\sigma_{xx} = \frac{3}{16}\rho g H^2 \cos^2\theta + \frac{1}{16}\rho g H^2 \sin^2\theta \tag{17}$$

$$\sigma_{yy} = \frac{3}{16}\rho g H^2 \sin^2\theta + \frac{1}{16}\rho g H^2 \cos^2\theta \tag{18}$$

$$\tau_{xy} = \tau_{yx} = \frac{1}{16}\rho g H^2 \sin 2\theta \tag{19}$$

and c is the friction coefficient and $k = 2\pi/L$ is the wave number.

Assuming that

$$\eta + d \cong d \tag{20}$$

and defining a stream friction Ψ such that

$$\frac{\partial \Psi}{\partial y} = - ud \tag{21}$$

$$\frac{\partial \Psi}{\partial x} = + vd, \tag{22}$$

automatically satisfies the continuity requirement. Cross-differentiating Eqs. (11) and (12) and utilizing (21) and (22) produces the governing circulation equation

$$\frac{\partial^2 \Psi}{\partial x^2} + \frac{\partial^2 \Psi}{\partial y^2} + \frac{\frac{\partial F}{\partial y}}{F}\frac{\partial \Psi}{\partial y} + \frac{\frac{\partial F}{\partial x}}{F}\frac{\partial \Psi}{\partial x} =$$

$$\frac{g}{F}\left\{\frac{\partial}{\partial y}\left[\frac{1}{d}\left(\frac{\partial \bar{\sigma}_{xx}}{\partial x} + \frac{\partial \bar{\tau}_{xy}}{\partial y}\right)\right] - \frac{\partial}{\partial x}\left[\frac{1}{d}\left(\frac{\partial \bar{\sigma}_{yy}}{\partial y} + \frac{\partial \bar{\tau}_{xy}}{\partial x}\right)\right]\right\} \tag{23}$$

where

$$F = \frac{2cH}{d^2 T \sinh kd} \tag{24}$$

$$\bar{\sigma}_{xx} = H^2 \left(\frac{3}{16}\cos^2\theta + \frac{1}{16}\sin^2\theta\right) \tag{25}$$

$$\bar{\sigma}_{yy} = H^2 \left(\frac{3}{16} \sin^2\theta + \frac{1}{16} \cos^2\theta\right) \tag{26}$$

$$\bar{\tau}_{xy} = \bar{\tau}_{yx} = \frac{1}{16} H^2 \sin 2\theta \tag{27}$$

NUMERICAL COMPUTATION

To initiate the computation, the bottom topography must be everywhere defined. An examination of the field data from Sonu (6), Figure 5 indicates that an approximate analytic representation can be obtained by the relationship

$$d(x,y) = 0.025x\left[1 + 20e^{-3\left(\frac{x}{20}\right)^{1/3}} \sin^{10}\left(\frac{\pi y}{80}\right)\right] \tag{28}$$

This produces a straight beach line (y-axis) and a periodic rip - current channel decaying exponentally offshore into a plane beach.

The first case to be analyzed is that of normal wave incidence. The computation proceeds by tracking the rays or orthogonals from deeper water where Shell's law is valid into the area defined by Eq. (28). Figure 3 indicates the rays on one-half of the periodic beach since the solution is symmetrical about the line $y=0$. The dotted line indicates the position of wave breaking and notice that a caustic occurs as the wave rays merge. While the "geometric optics" approximation breaks down near a caustic, the wave has already broken so that the wave height computation is determined from Eq. 10. The kinematical equations (1) to (3) still produce results independent of the caustic and these are assumed sufficient to provide wave direction data.

Following the ray solution, a algorithm is utilized to transform the essentially "random" locations of wave height and direction into a uniform grid by a two-dimensional interpolation scheme. The grid data is then used to solve Eq. 23 by application of a Gauss-Seidel relaxation algorithm with the boundary conditions.

$$\psi = 0 \text{ at } y = 0 \text{ and } y = 40 \text{ meters}$$

$$\psi = 0 \text{ at } x = 0 \text{ and } x = 385 \text{ meters}$$

The final stream line solution for normal incidence is shown in Figure 4. As a test case, a full period of 80 meters was used and the results were identical with Figure 4 with similar stream line patterns mirror imaged about $y = 0$ and 40 meters except that these streamlines are negative in value. While qualitatively the results are reasonable, quantitatively the maximum rip - current velocity is about 4 meters/second. This seems to be much larger than existing prototype measurements from Sonu (6), Figure 5.

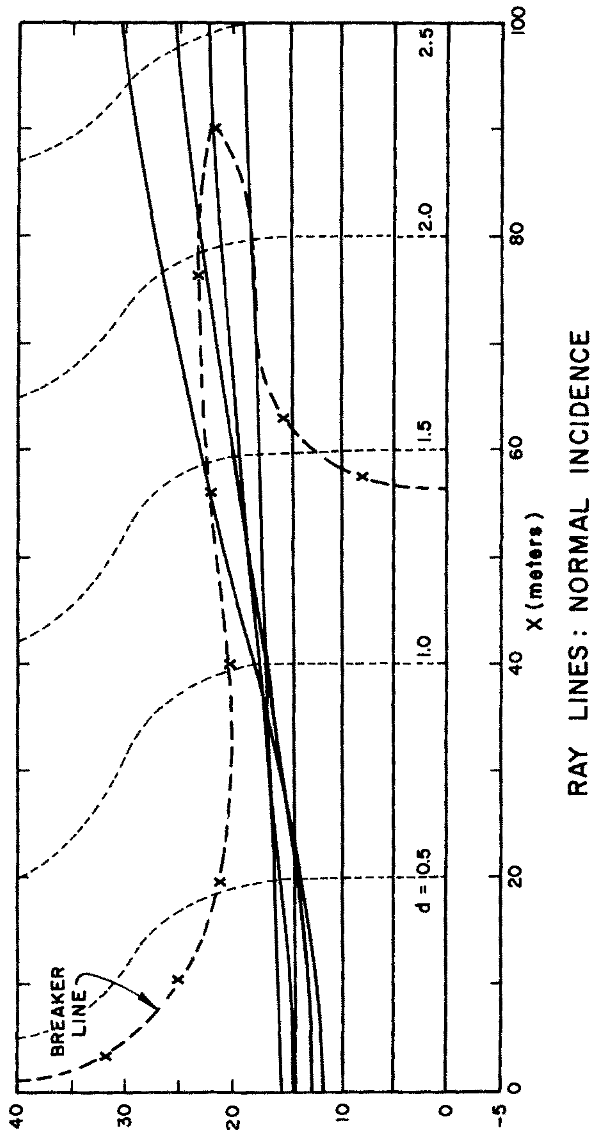

Figure 3: Schematic View of Wave Orthagonals with Normal Incidence

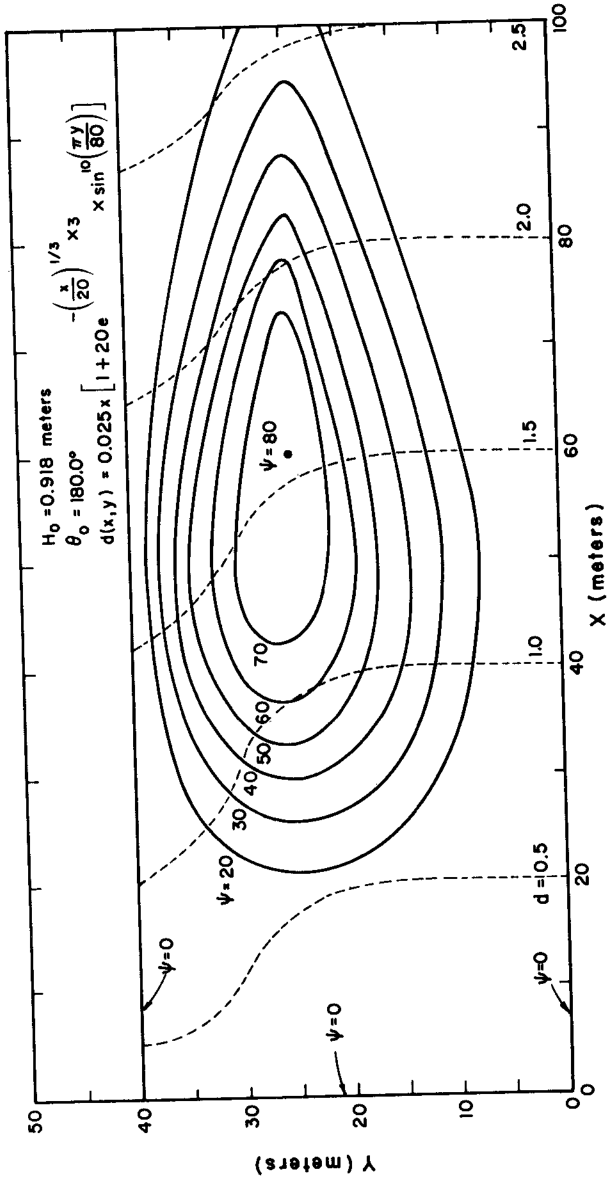

NORMAL INCIDENCE

Figure 4: Numerical Stream Function Solution with Normal Wave Incidence

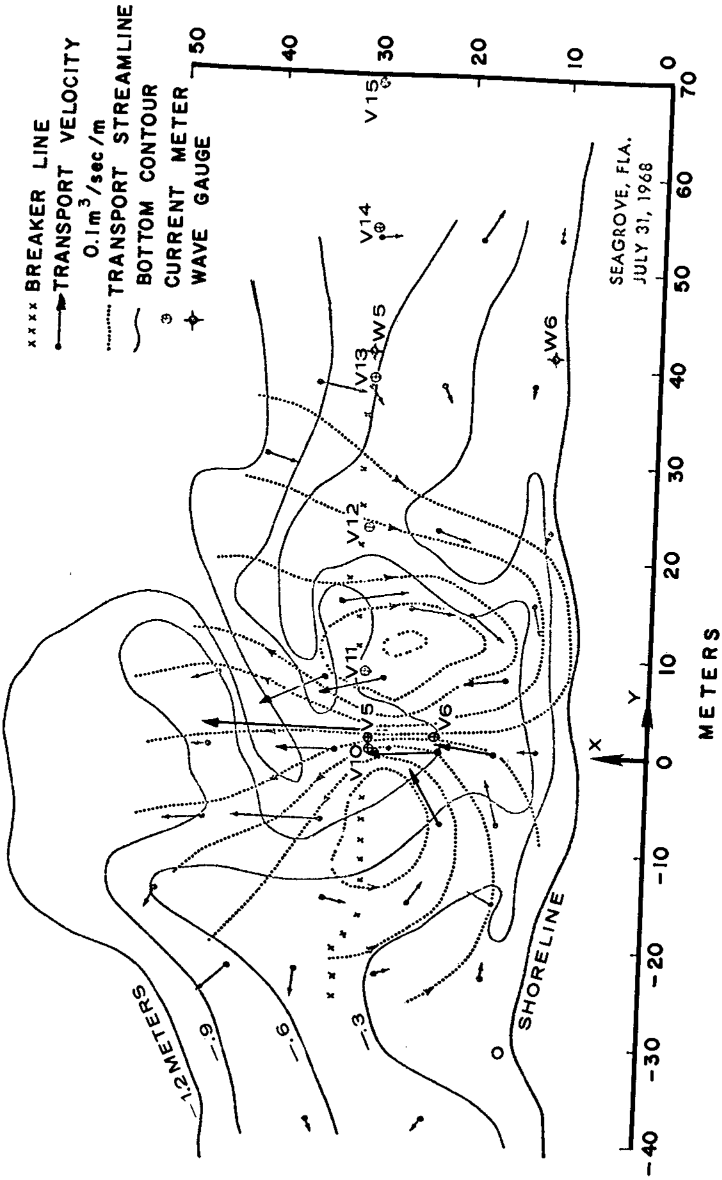

Figure 5: Distribution of Transport Velocities and Streamlines in a Circulation Cell. Streamline Separation is 0.4m³ (sec, H_b = 0.395 meters, T_b = 5 sec [From Sonu (6)]

The next case examined was that of wave attack at an oblique angle to the shore line. For this case, a deep water angle and wave height of

$$\theta_o = 153^o, \ H_o = 1.0 \text{ meters}$$

was used. Typical rays are described in Figure 6 with the associated breaker line. In this problem while the shore line and off-shore boundary conditions are well defined as

$$\psi = 0 \text{ at } x = 0 \text{ and } x = 385 \text{ meters}$$

the longshore boundary conditions are as yet unknown. Since this is a boundary value problem, the longshore ψ conditions must be apriori constrained before a solution can be found. To solve this problem, the numerical relaxation algorithm was allowed to update ψ along the line $y = 0$ and the periodic condition was imposed that

$$\psi(x, y=80) = \psi(x, y=0)$$

Convergence for this case required about 700 iterations since the imposed accuracy was very high. The solution for the stream function field is shown in Figure 7. Notice the existance of a small negative area of ψ which is a degeneration of the previously described negative cell produced by normal wave incidence.

An examination of the prototype field data from Sonu (6) Figure 8 indicates a optimistic qualitative agreement. Quantitatively the numerically computed maximum rip - current velocities are about 4 meters/second which is much larger than observed values. Also, notice that the incoming rip - current velocity is of the same magnitude as the outgoing velocity which is not observed in the field and also the maximum rip velocity direction is oblique to the imposed bottom topography.

RESULTS AND CONCLUSIONS

As previously indicated, while the analysis for normal wave incidence Figure 4 yields qualitatively reasonable results, quantitative estimates of the rip - current velocity are much larger than field measurements. An examination of Figure 3 shows that in the channel area the breaker line extends almost to the shoreline at $y = 40$ meters and out to $x = 90$ meters at $y = 20$ meters. Examining Figure 5, the field data does not indicate this large variation in the breaker line and consequently this suggests that there may be a strong wave-current interaction which would produce a more uniform breaker line. Since this effect would yield a more uniform longitudional wave height distribution, it is expected that the rip - current velocity would be greatly reduced. The analysis for wave-current interaction has been completed and the numerical algorithm generated although presently no results are available.

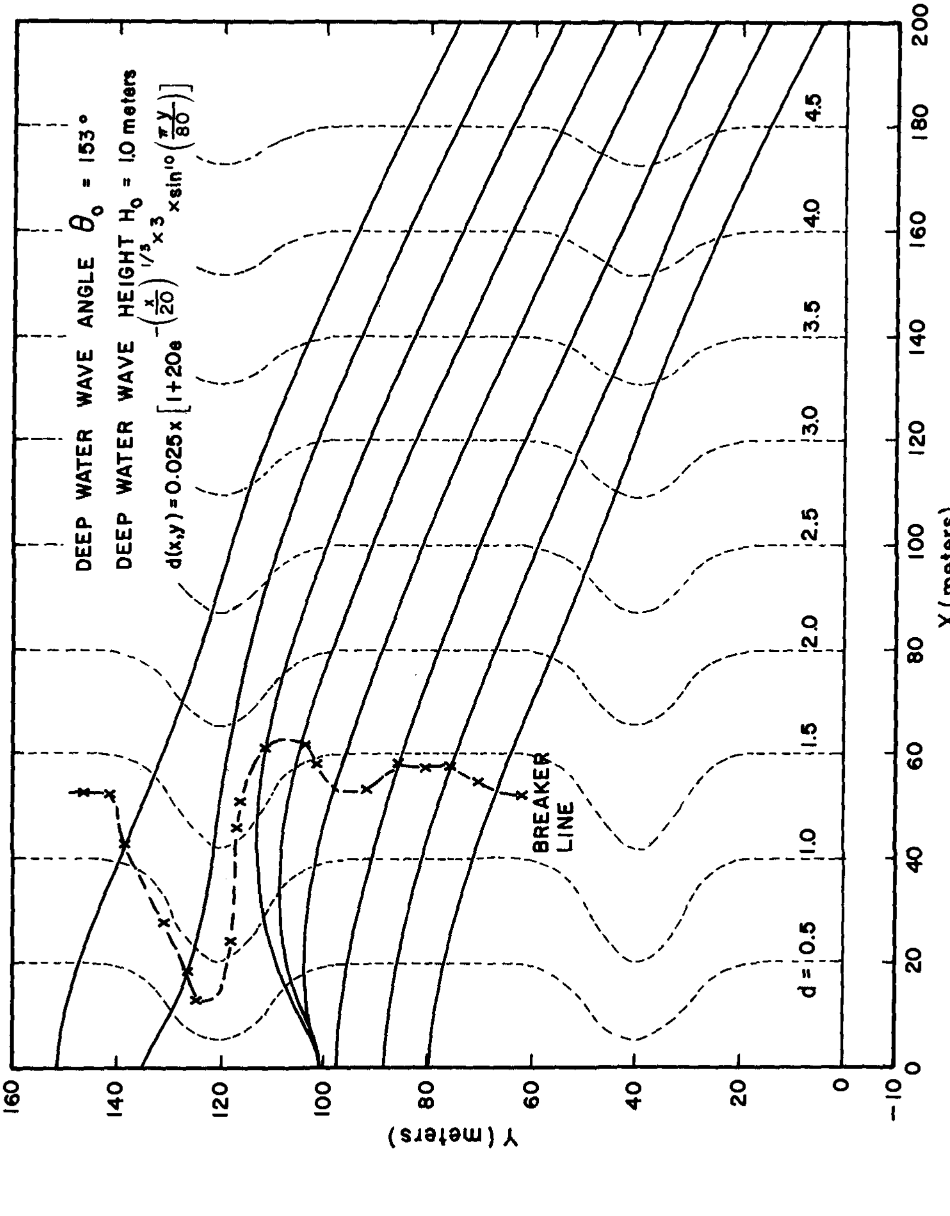

Figure 6: Wave Orthagonals for Oblique Incidence

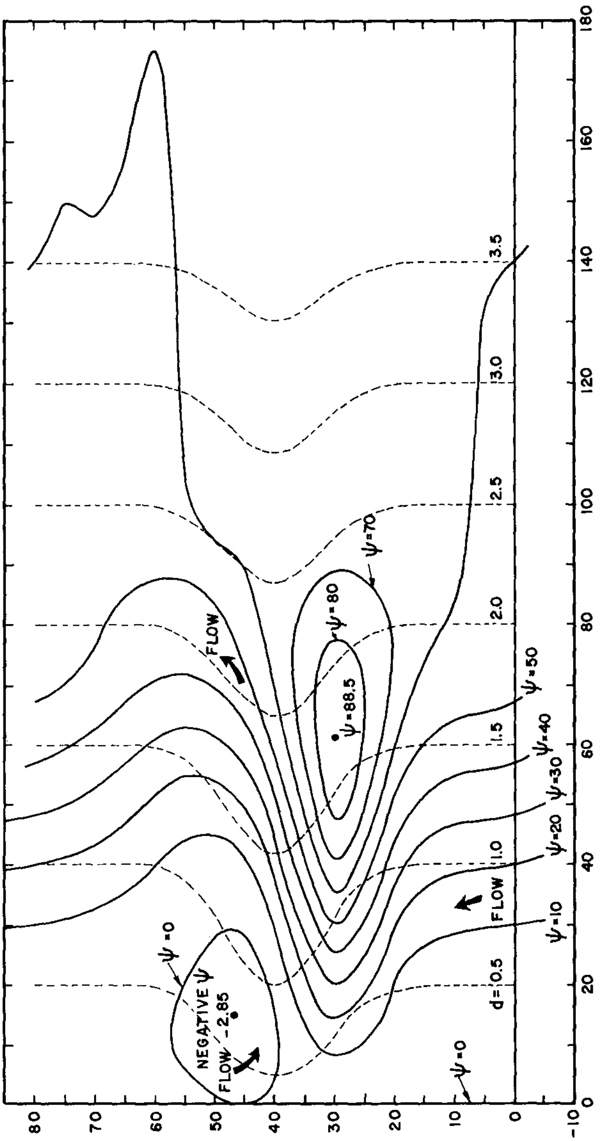

Figure 7: Numerical Stream Function Solution for Oblique Incidence

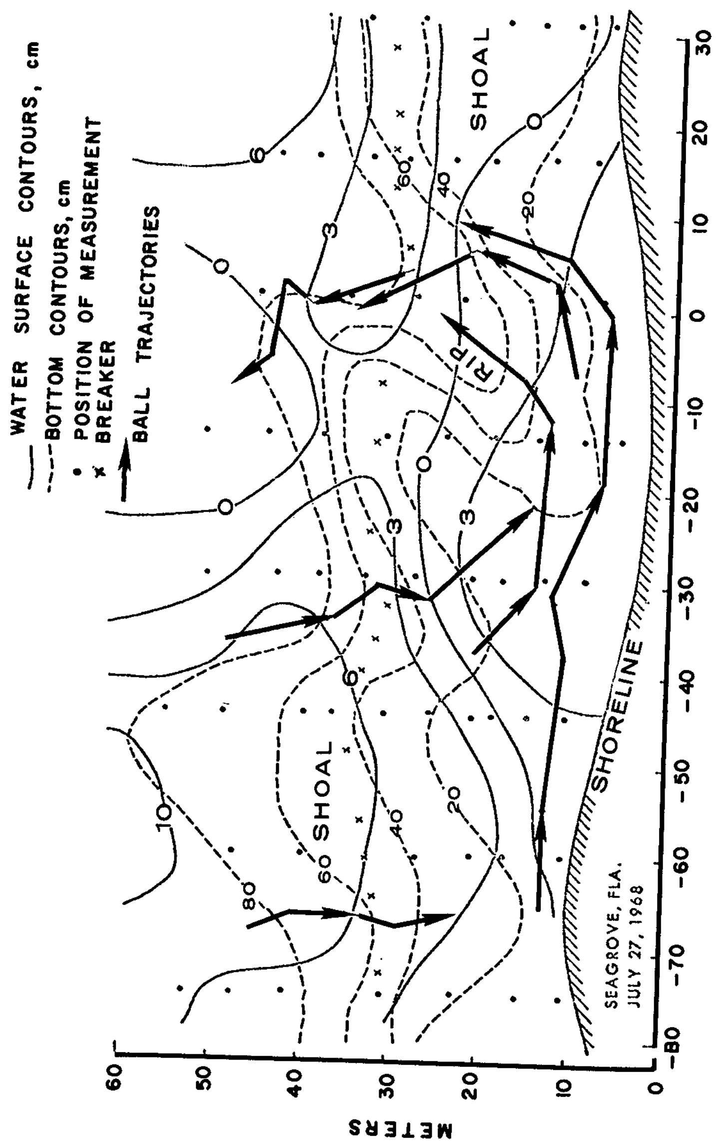

Figure 8: Nearshore Circulation due to Oblique Incidence [From Sonu (6)]

The case of oblique wave attack again yields much larger velocities than field data. Since the field data Figure 8 shows a definite skewing of the rip - channel in line with the current vector, the following depth configuration was recently imposed

$$d(k,y) = 0.025x\,[1 + 20e^{-3\left(\frac{x}{20}\right)^{1/3}} \sin^{10} \frac{\pi}{80}\,(y - x\tan\alpha)] \tag{29}$$

where $\alpha = 30^{\circ}$. This depth function effectively skewed the rip - channel 30° to the x-axis and performing the ray computations through the relaxation procedure produced a solution very similar to Figure 8 except that now the maximum rip - current velocity was about 1.8 meters/second and the incoming rip - current velocity was much smaller than the outgoing velocity. This then indicates the importance of the bottom topography and also shows that such a profile as given by Eq. (28) would probably be scowed by oblique waves and possibly produce a bottom profile similar to Eq. (29). Unfortunately at press time a graphical display of the stream function solution to Eq. (29) is not available.

The previously described results is part of a continuing research effort to describe the hydrodynamic and littoral nearshore environment. The preliminary results herein are very optimistic and indicate that the local bottom configuration may be very important in the determination of the nearshore wave-induced circulation pattern.

ACKNOWLEDGMENT

This study was sponsored by the Office of Naval Research, Geography Programs under Contract No. N00014-69-C-0107. The author would like to express appreciation to Dr. J. Ian Collins for stimulating discussions and to Mr. Wayne Wier for valuable computer programing services.

REFERENCES

1. Bowen, A.J. (1969), "Rip Currents, 1, Theoretical Investigation", Journal of Geoghys. Res., No. 74, Vol. 23, pp. 5467-5478.

2. LeMéhauté, B. and Koh, R. C.Y. (1967), "On the Breaking of Waves Arriving at an Angle to the Shore", Journel of Hyd. Res., No. 1, Vol. 5, pp. 67-88.

3. Longuet-Higgins, M.S. and Stewart, R.W. (1964), "Radiation Stress in Water Waves, a Physical Discussion with Application", Deep Sea Research, No. 11, Vol. 4, pp. 529-563.

4. Miche, R. (1944), "Mouvements Ondulatoires de la Mer en Profondeur Constante ou Décroissante", Ann. des Ponts et.

5. Munk, W.H. and Arthur, R.S. (1951), "Wave Intensity along a Refracted Wave", Circular 521, U.S. Dept. of Commerce, National Bureau of Standards, pp. 95-108.

6. Sonu, C.J. (1972), "Field Observations of Nearshore Circulation and Meandering Currents", J. of Geophys. Res., Oceans and Atms., No. 18, Vol. 77, pp. 3232-3247.